

# Bias with a Timer: Axion Domain Wall Decay and Dark Matter

Sally Yuxuan Hao,<sup>1,2</sup> Shota Nakagawa,<sup>1,2</sup> Yuichiro Nakai,<sup>1,2</sup> and Motoo Suzuki<sup>3,4,5</sup>

<sup>1</sup>*Tsung-Dao Lee Institute, Shanghai Jiao Tong University,  
No. 1 Lisuo Road, Pudong New Area, Shanghai 201210, China*  
<sup>2</sup>*School of Physics and Astronomy, Shanghai Jiao Tong University,  
800 Dongchuan Road, Shanghai 200240, China*

<sup>3</sup>*SISSA International School for Advanced Studies, Via Bonomea 265, 34136, Trieste, Italy*

<sup>4</sup>*INFN, Sezione di Trieste, Via Valerio 2, 34127, Italy*

<sup>5</sup>*IFPU, Institute for Fundamental Physics of the Universe, Via Beirut 2, 34014 Trieste, Italy*

We explore the interplay of the post-inflationary QCD axion and a light scalar field for the axion domain wall decay and dark matter (DM). The scalar field possesses a nonzero vacuum expectation value (VEV) during inflation, so that its interaction with the axion effectively serves as an explicit Peccei-Quinn (PQ) violating term. At a temperature below the PQ phase transition, the effective PQ violating interaction generates the axion potential which generally contains multiple degenerate vacua leading to the formation of the axion string-domain wall networks. The following QCD phase transition provides another contribution to the axion potential making domain walls decay before they dominate the Universe. Later, the scalar field starts to relax to the minimum of its potential with a vanishing VEV, turning off the effective PQ violating interaction so that the axion potential is aligned with the QCD vacuum. We keep track of the evolution of the axion-scalar system and discuss the production of the axion DM through the domain wall decay and the (trapped) misalignment. We find that the string-wall network in some cases can decay due to its structural instability, rather than the volume pressure, and the correct axion DM abundance is realized with the decay constant larger than that of the conventional post-inflationary QCD axion without fine tuning.

## I. INTRODUCTION

The strong CP problem remains one of the most important puzzles in the Standard Model. Although Quantum Chromodynamics (QCD) allows a CP-violating  $\theta$ -term in its Lagrangian, experimental limits on the electric dipole moment (EDM) of the neutron require the physical strong CP phase  $\bar{\theta}$  to be unnaturally small,  $|\bar{\theta}| \lesssim 10^{-10}$  [1, 2]. This tension between the theoretical expectation and observational constraints constitutes the strong CP problem.

A particularly elegant solution to the strong CP problem is provided by the Peccei-Quinn (PQ) mechanism [3], which promotes the parameter  $\bar{\theta}$  to a dynamical field by introducing a new global  $U(1)$  symmetry, spontaneously broken at some high energy scale. The associated pseudo-Nambu-Goldstone boson, the axion [4, 5], dynamically relaxes  $\bar{\theta}$  to zero. Remarkably, the axion also serves as a promising candidate for cold dark matter (DM). Axion DM can be produced through several mechanisms, depending on the cosmological history and the scale of the PQ symmetry breaking. The most well-known is the misalignment mechanism [6–8], in which the axion field, initially displaced from the minimum of its potential, begins to oscillate when the Hubble parameter drops below the (temperature dependent) axion mass. Such a coherent oscillation behaves like cold DM. In the post-inflationary scenario where the PQ symmetry is broken after inflation, spatial variations in the initial axion field lead to the formation of topological defects, such as global strings and domain walls, which also contribute to the axion DM abundance through their decays.

In the present paper, we study a cosmological scenario

in which the post-inflationary QCD axion interacts with a light scalar field, resulting in a dynamically controlled mechanism for the axion domain wall decay and DM production. The introduced scalar field acquires a nonzero vacuum expectation value (VEV) during inflation, which induces an effective PQ symmetry breaking interaction through its coupling to the axion field. As the Universe cools after the PQ symmetry is spontaneously broken, the effective interaction generates an axion potential with multiple degenerate minima, leading to the formation of a network of the axion strings and domain walls. Subsequently, the QCD phase transition generates an additional contribution to the axion potential, which breaks the vacuum degeneracy and triggers the decay of the domain walls before they dominate the energy density of the Universe. We newly point out that the string-wall network in some cases can decay due to its structural instability, rather than the volume pressure. At a later time, the scalar field evolves to the minimum of its potential, where its VEV vanishes. This turns off the effective PQ breaking interaction and leaves the axion potential aligned with the CP-conserving QCD vacuum, thereby preserving the solution to the strong CP problem.

Our model is similar to that presented in ref. [9] where the axion potential, generated by the effective PQ breaking interaction of the scalar field, does not contain multiple degenerate minima unlike our model, so that DM production through the domain wall decay is negligible. In addition, ref. [9] have simply assumed that the evolution of the axion never backreacts that of the new scalar field. Instead, the present paper comprehensively investigates and presents the evolution of the axion-scalar system and the resulting axion DM abundance, which re-

ceives contributions from both the domain wall decay and the misalignment mechanism. We also discuss the importance of the trapping effect of the axion field [10–18] due to the effective PQ breaking interaction for the estimation of the misalignment contribution. It is found that the correct DM abundance is realized with the axion decay constant larger than that of the conventional post-inflationary QCD axion without fine tuning.

The rest of the paper is organized as follows. In section II, we present our setup and describe the evolution of the newly introduced scalar field and the PQ breaking field. Section III discusses the axion potential and the dynamics of the axion-scalar system. Then, in section IV, we explore the evolution of the axion string-domain wall network. The DM abundance is estimated in section V. We outline a possible UV completion in section VI. Section VII is devoted to conclusions and discussions.

## II. PQ MECHANISM WITH A SPECTATOR

We consider a PQ breaking scalar field, which contains the axion for the PQ mechanism, interacting with a light complex scalar, called a spectator field [9]. After presenting the setup, we review the evolution of the PQ field and the spectator field.

### A. Setup

Let us introduce a spectator complex scalar field  $S$ , which interacts with the conventional PQ scalar field  $P$  with PQ charge 1. Their potential is given by<sup>1</sup>

$$V_{\text{PQ}}(P, S) \supset \lambda_P \left( |P|^2 - \frac{v_{\text{PQ}}^2}{2} \right)^2 + \frac{1}{(n!)^2} \frac{\lambda_S^2}{M_{\text{Pl}}^{2n-4}} |S|^{2n} + m_S^2 |S|^2 + \left( \frac{\lambda}{m! \ell! M_{\text{Pl}}^{m+\ell-4}} S^m P^\ell + \text{h.c.} \right), \quad (1)$$

where  $v_{\text{PQ}}$  represents the breaking scale of the PQ symmetry,  $m_S$  is a mass parameter,  $\lambda_P, \lambda_S, \lambda$  are dimensionless coupling coefficients, and  $M_{\text{Pl}} \equiv 1/\sqrt{8\pi G}$  with the Newton constant  $G$ . The mass parameter  $m_S$  is assumed to be small so that it becomes relevant after the QCD phase transition. One can assign the PQ charge  $-\ell/m$  ( $m, \ell \in \mathbb{N}$ ) for the spectator field  $S$  to respect the PQ symmetry. Throughout the paper, we assume that  $n$  ( $\in \mathbb{N}$ ) is larger than or equal to 5. We will discuss how other lower dimensional operators are suppressed in Sec. VI. When  $S$  has a large field value, the evolution of  $P$  can be affected significantly due to the mixing interaction.

The PQ breaking field  $P$  and the spectator field  $S$  interact with the inflaton field  $\phi$ ,

$$V_{\text{PQ}} \supset V_{\text{inf}}(\phi) + \frac{c_P}{3} \frac{V_{\text{inf}}(\phi)}{M_{\text{Pl}}^2} |P|^2 - \frac{c_S}{3} \frac{V_{\text{inf}}(\phi)}{M_{\text{Pl}}^2} |S|^2. \quad (2)$$

Here  $V_{\text{inf}}$  is the inflaton potential, and  $c_P, c_S$  are taken to be positive constants. The interaction terms with the inflaton respectively lead to positive and negative mass terms to  $P$  and  $S$  during inflation.

We ignore the finite temperature correction to the potential of  $S$ . This can be justified when the inflaton decays dominantly to the Standard Model sector, and  $S$  is never thermalized by the tiny mixing with  $P$ . We also note that this scenario is applicable to any specific axion models, such as KSVZ [19, 20] and DFSZ [21, 22] models.

### B. Evolution of the spectator field

The interaction terms in Eqs. (1), (2) induce a large expectation value  $\langle S \rangle$  from inflationary epoch to radiation-dominated era [9, 23]. Following ref. [9], we summarize the analytic formula of  $\langle S \rangle$  for each epoch.

During inflation,  $V_{\text{inf}} \simeq 3H_{\text{inf}}^2 M_{\text{Pl}}^2$  with  $H_{\text{inf}}$  the Hubble parameter during inflation, and  $S$  has a negative Hubble mass term,

$$V(S) \simeq \frac{1}{(n!)^2} \frac{\lambda_S^2}{M_{\text{Pl}}^{2n-4}} |S|^{2n} - c_S H_{\text{inf}}^2 |S|^2. \quad (3)$$

Here we assume that the mixing term is negligibly small compared to these terms. The expectation value is estimated at the potential minimum,

$$\langle S_{\text{inf}} \rangle \simeq \left( \sqrt{\frac{c_S}{n}} \frac{n!}{\lambda_S} \right)^{\frac{1}{n-1}} \left( \frac{H_{\text{inf}}}{M_{\text{Pl}}} \right)^{\frac{1}{n-1}} M_{\text{Pl}}. \quad (4)$$

For example,  $\langle S_{\text{inf}} \rangle \sim M_{\text{Pl}}$  for  $H_{\text{inf}} = 10^{12}$  GeV,  $n = 6$ ,  $c_S = 1$ , and  $\lambda_S = 10^{-4}$ , which means that  $\lambda_S \gtrsim 10^{-4}$  for a sub-Planckian VEV of  $S$ . The large field value during inflation suppresses the isocurvature bound. As will be discussed in Sec. V, we can also take  $\lambda_S \sim 1$  to suppress the isocurvature bound sufficiently, but as a more conservative value, we take  $\lambda_S = 10^{-4}$  throughout the paper, which does not change any overall consequences.

After inflation, the inflaton oscillation dominates the energy density in the Universe. Since the inflaton oscillates with a time scale shorter than the Hubble time,  $S$  evolves with the time-averaged inflaton potential,

$$\bar{V}_{\text{inf}} \simeq \frac{3}{2} H^2 M_{\text{Pl}}^2. \quad (5)$$

The equation of motion for  $S$  is given by

$$|\ddot{S}| + 3H|\dot{S}| + \frac{n\lambda_S^2}{(n!)^2 M_{\text{Pl}}^{2n-4}} |S|^{2n-1} - \frac{c_S}{2} H^2 |S| = 0, \quad (6)$$

<sup>1</sup> We generalize the mixing term with  $\ell = 1$  introduced in ref. [9].

where the dot denotes the derivative with respect to cosmic time  $t$ . We neglect the phase direction of  $S$  approximately, as long as  $m \gg \ell$ , so that any motion is only slightly induced in the phase direction. Following the method described in ref. [9], we obtain a large expectation value of  $S$  during inflaton domination,

$$\langle |S_{\text{ID}}| \rangle \simeq \left( \sqrt{\frac{c_S}{n}} \frac{n!}{\lambda_S} \right)^{\frac{1}{n-1}} \left( \frac{H}{M_{\text{Pl}}} \right)^{\frac{1}{n-1}} M_{\text{Pl}}. \quad (7)$$

This behavior is known as the scaling solution [24].

After reheating, the Universe undergoes the radiation dominated era. Since  $S$  no longer feels the inflaton coupling, the equation of motion of  $S$  is given by

$$|\ddot{S}| + 3H|\dot{S}| + \frac{n\lambda_S^2}{(n!)^2 M_{\text{Pl}}^{2n-4}} |S|^{2n-1} = 0. \quad (8)$$

We then obtain a value of  $S$  during the radiation dominated era for  $n \geq 6$  [23],

$$\langle |S_{\text{RD}}| \rangle \simeq \left[ \frac{2(n-3)(n!)^2}{n(n-1)^2 \lambda_S^2} \right]^{\frac{1}{2(n-1)}} \left( \frac{H}{M_{\text{Pl}}} \right)^{\frac{1}{n-1}} M_{\text{Pl}}. \quad (9)$$

Note that the case of  $n = 5$  also leads to a large value of  $S$ , but its behavior is different and more complicated. Thus, we choose  $n = 6$  as a reference value throughout the present paper.<sup>2</sup>

Throughout the history in the Universe until the oscillation of  $S$  starts, the spectator field has a large field value (4), (7), and (9), leading to a large PQ breaking potential via the mixing term in Eq. (1). When  $m_S \sim H$ ,  $S$  starts to oscillate around its origin, so that the PQ breaking effect is suppressed and becomes small enough to evade the experimental bound of the neutron EDM. Since we focus on the case where the PQ breaking is effective in the axion evolution until the QCD confinement, we assume the range of the mass parameter,

$$m_S \lesssim \sqrt{\frac{\pi^2 g_*}{90}} \frac{\Lambda_{\text{QCD}}^2}{M_{\text{Pl}}} \simeq 3 \times 10^{-11} \text{ eV}, \quad (10)$$

where  $\Lambda_{\text{QCD}} \simeq 150 \text{ MeV}$  denotes the dynamical scale of QCD. Note that the abundance of coherent oscillation of  $S$  is negligibly small for this mass range.

### C. Evolution of the PQ field

During inflation, the potential of  $P$  is described by

$$V_P = (c_P H_{\text{inf}}^2 - \lambda_P v_{\text{PQ}}^2) |P|^2 + \lambda_P |P|^4 + \frac{\lambda}{m! \ell! M_{\text{Pl}}^{m+\ell-4}} \langle S_{\text{inf}} \rangle^m P^\ell + \text{c.c.}, \quad (11)$$

<sup>2</sup> Likewise,  $S$  obeys the scaling solution in the matter-dominated Universe, given by  $\langle S_{\text{MD}} \rangle \simeq \langle S_{\text{RD}} \rangle \times (9(n-2)/8(n-3))^{1/(2n-2)}$ , which corresponds to the case with  $m_S \lesssim 10^{-28} \text{ eV}$ .

where the quadratic term is positive, assuming  $H_{\text{inf}} \gg v_{\text{PQ}}$ , and thus, the minimum of  $P$  depends on the latter two terms.<sup>3</sup>

When the Universe reheats,  $P$  acquires a thermal potential due to its coupling to the thermal bath. For instance, in the KSVZ model, it is given by the coupling to PQ-charged quarks. As the Universe cools, the effect of the thermal potential gets smaller, and at  $T \sim v_{\text{PQ}}$ , the PQ symmetry is spontaneously broken, so that an axion appears in the low-energy effective theory.

## III. EFFECTS OF PQ BREAKING

We now discuss the effective axion potential generated from the mixing term in Eq. (1) and the non-perturbative QCD effect, and investigate the dynamics of the axion-spectator field system.

### A. Effective axion potential

The mixing interaction gives rise to an effective potential of the axion, as long as  $S$  keeps a large VEV. After the PQ symmetry is spontaneously broken, we parameterize the PQ field and the spectator field by

$$P = \frac{v_{\text{PQ}}}{\sqrt{2}} e^{ia/v_{\text{PQ}}}, \quad S = \frac{\chi}{\sqrt{2}} e^{ib/\chi}, \quad (12)$$

to obtain the potential,

$$V_{\text{PQ}} \simeq -\frac{1}{\ell^2} m_{\text{PQ}}^2 v_{\text{PQ}}^2 \cos \left( \ell \frac{a}{v_{\text{PQ}}} + m \frac{b}{\chi} + \delta \right). \quad (13)$$

Here  $\delta$  denotes a constant phase of  $\lambda$ , and the corresponding mass for the axion is defined as

$$m_{\text{PQ}}^2(T) \simeq \frac{|\lambda| \ell^2}{2^{\ell/2-1} m! \ell!} \frac{\langle S_{\text{RD}} \rangle^m v_{\text{PQ}}^{\ell-2}}{M_{\text{Pl}}^{m+\ell-4}}. \quad (14)$$

Note that the Lagrangian is PQ symmetric, but the potential effectively breaks the PQ symmetry for a nonzero value of  $S$ .

In addition to the mixing interaction, the axion acquires a potential via non-perturbative effects of QCD,

$$V_{\text{QCD}}(a) = m_a^2(T) f_a^2 \left( 1 - \cos \frac{a}{f_a} \right), \quad (15)$$

<sup>3</sup> There is a single minimum at the origin,  $\langle P_{\text{inf}} \rangle \simeq 0$ , for even values of  $\ell$ . On the other hand, when  $\ell$  is odd, the analysis depends on  $\ell$ . For  $\ell = 1$ , a single minimum deviates from the origin due to the linear term. For  $\ell = 3$ , there are two minima. For  $\ell = 5, 7, 9, \dots$ , the potential has a single minimum but is not bounded from below, which requires an additional higher dimensional ( $> \ell$ ) potential. Here, the phase direction is assumed to be stabilized at the origin for simplicity.

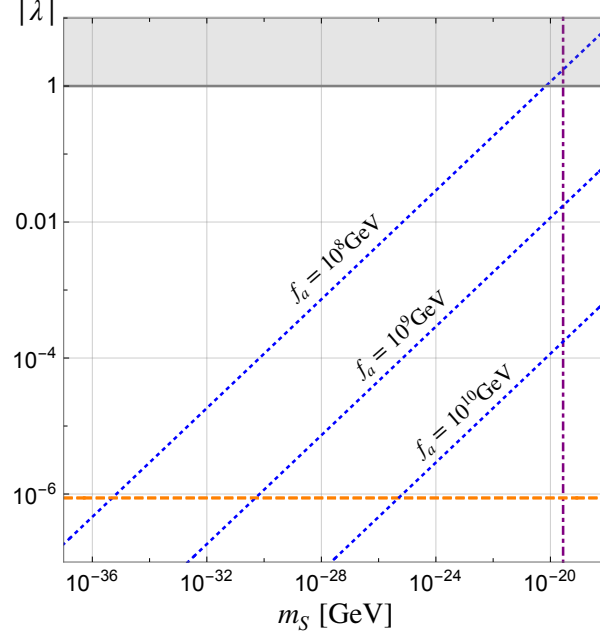


FIG. 1. The parameter space in the  $(m_S, |\lambda|)$  plane. The blue dotted lines show the constraint (22) for various  $f_a$ . The backreaction is not negligible in the region above each line. The orange dashed lines correspond to the constraint  $T_{\text{osc}} > T_{\text{osc}}^{(\text{conv})}$ . The region above each line satisfies the constraint. The purple dot-dashed line represents the upper bound on  $m_S$  of our interest (10). The gray shaded region corresponds to  $|\lambda| > 1$ . For  $\lambda_S = 10^{-4}$ , we set  $(N_{\text{DW}}, \ell, m, n) = (3, 2, 10, 6)$ .

where we define  $f_a \equiv v_{\text{PQ}}/N_{\text{DW}}$  as the axion decay constant with  $N_{\text{DW}}$  the domain wall number. We refer to the lattice results [25] for the temperature-dependent axion mass,  $m_a(T)$  for  $T \gtrsim \Lambda_{\text{QCD}}$ , given by

$$m_a(T) \simeq m_{a,0} \left( \frac{T}{\Lambda_{\text{QCD}}} \right)^{-\tilde{b}}, \quad (16)$$

with a numerical exponent  $\tilde{b} = 3.92$ .<sup>4</sup> Here  $m_{a,0}$  is defined as the zero temperature mass for  $T \lesssim \Lambda_{\text{QCD}}$ . By the chiral perturbation theory [26, 27], the mass is estimated as

$$m_{a,0} \simeq 0.57 \text{ MeV} \left( \frac{10^{10} \text{ GeV}}{f_a} \right). \quad (17)$$

Since the potential (13) can be dominant over the usual one (15) before the QCD confinement, it affects the axion dynamics in a nontrivial way. Our focus is on a scenario that the QCD axion starts to oscillate earlier than the conventional onset of oscillation,  $T_{\text{osc}} \gg T_{\text{osc}}^{(\text{conv})}$  which is estimated by  $H \sim m_a$ ,

$$T_{\text{osc}}^{(\text{conv})} \simeq 2.6 \text{ GeV} \left( \frac{g_*}{80} \right)^{-0.084} \left( \frac{f_a}{10^{10} \text{ GeV}} \right)^{-0.17}. \quad (18)$$

Due to the dependence of  $m_{\text{PQ}}$  on  $m$ , we consider two cases: (i)  $m \geq 2n - 2$  and (ii)  $m \leq 2n - 3$ .

<sup>4</sup> We use the same function of the axion mass as that of ref. [16].

(i)  $m \geq 2n - 2$

Since  $m_{\text{PQ}} \propto H^{m/(2n-2)}$ , it decreases faster than or at the same rate with the Hubble parameter. The condition  $T_{\text{osc}} \gg T_{\text{osc}}^{(\text{conv})}$  is satisfied, as long as  $H \lesssim m_{\text{PQ}}$  at the PQ breaking scale so that we have

$$|\lambda| > \frac{2^{\ell/2-1} m! \ell! \pi^2 g_*}{\ell^2 90} \left( \frac{v_{\text{PQ}}}{M_{\text{Pl}}} \right)^{6-\ell} \left( \frac{\langle S_{\text{RD}} \rangle}{M_{\text{Pl}}} \right)^{-m}. \quad (19)$$

Thus,  $T_{\text{osc}} \simeq v_{\text{PQ}}$ . Note that a larger exponent  $m$  of the mixing term requires a larger value of  $|\lambda|$  due to this constraint. In fact, we find that there is no allowed region for  $m \geq 2n$ , i.e.,  $|\lambda|$  is much larger than one for  $n = 6$ , when taking  $\ell > 1$  we are interested in. In the next section, we will see that the case of  $m = 2n - 1$  is also restricted. Then, we only consider  $m = 2n - 2$ . As will be discussed later, the domain wall density in the scaling scheme is estimated by  $\rho_{\text{wall}} \sim m_{\text{PQ}} v_{\text{PQ}}^2 H \propto H^{m/(2n-2)+1}$ , so that the domain wall density dilutes at the same rate as the radiation for  $m = 2n - 2$ .

(ii)  $m \leq 2n - 3$

In this case,  $m_{\text{PQ}}$  decreases more slowly than  $H$ . The oscillation temperature is then given by

$$T_{\text{osc}} \simeq 20 \text{ TeV} \left( \frac{106.75}{g_*} \right)^{\frac{1}{4}} \left( \frac{f_a}{10^{10} \text{ GeV}} \right)^{\frac{5}{2}} \times \left( \frac{N_{\text{DW}}}{2} \right)^{\frac{5}{2}} \left( \frac{|\lambda|}{10^{-3}} \right)^{\frac{5}{2}} \left( \frac{\lambda_S}{10^{-4}} \right)^{-\frac{9}{2}}, \quad (20)$$

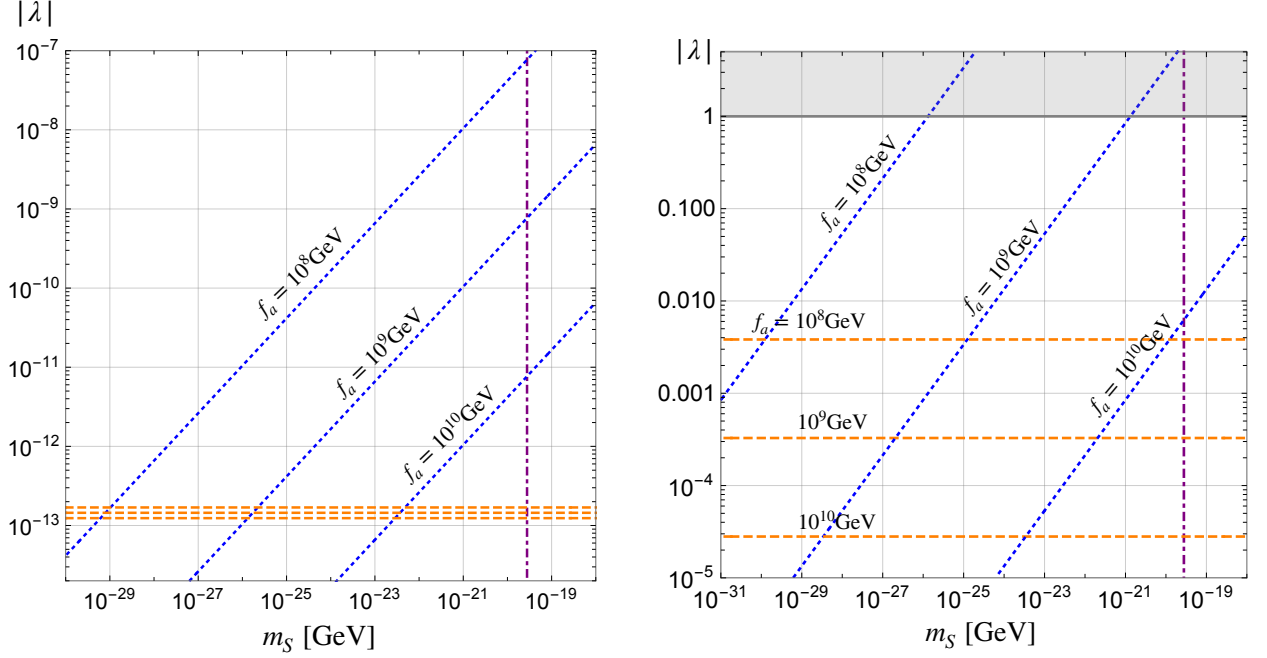


FIG. 2. The parameter space in the  $(m_S, |\lambda|)$  plane. For  $\lambda_S = 10^{-4}$ , we set  $(N_{\text{DW}}, \ell, m, n) = (3, 2, 9, 6)$  and  $(2, 3, 9, 6)$  in the left and right panels, respectively. See Fig. 1 for the description of lines. Note that the orange dashed lines in the left panel correspond to  $f_a = 10^8, 10^9, 10^{10}$  GeV from the above.

for  $T_{\text{osc}} < v_{\text{PQ}}$ , otherwise  $T_{\text{osc}} = v_{\text{PQ}}$ . Here we set  $\ell = 3$ ,  $m = 9$ , and  $n = 6$ . Solving  $T_{\text{osc}} \gg T_{\text{osc}}^{(\text{conv})}$ , we obtain the lower bound on  $|\lambda|$ . Since the domain wall density is proportional to  $H^{m/(2n-2)+1}$  with the exponent  $m/(2n-2)+1$  smaller than but close to 2, the domain wall cannot dominate the Universe until the QCD scale.

### B. Backreaction

So far, we have implicitly assumed that the evolution of  $P$  never backreacts that of  $S$  to simplify the analysis [9], which is justified by imposing a condition,

$$\frac{1}{(n!)^2} \frac{\lambda_S^2}{M_{\text{Pl}}^{2n-4}} |S|^{2n} > \frac{|\lambda|}{m! \ell! M_{\text{Pl}}^{m+\ell-4}} |S|^{m \ell} v_{\text{PQ}}^{\ell}, \quad (21)$$

at any temperature from the spontaneous breaking of the PQ symmetry to the onset of oscillation of  $S$ . We then obtain the upper bound on  $|\lambda|$ ,

$$|\lambda| < \frac{m! \ell! \lambda_S^2}{(n!)^2} \left( \frac{M_{\text{Pl}}}{v_{\text{PQ}}} \right)^{\ell} \left[ \frac{2(n-3)(n!)^2}{n(n-1)^2 \lambda_S^2} \frac{m_S^2}{M_{\text{Pl}}^2} \right]^{\frac{2n-m}{2(n-1)}}. \quad (22)$$

Let us summarize the parameter space  $(m_S, |\lambda|)$  with the constraints of  $T_{\text{osc}} > T_{\text{osc}}^{(\text{conv})}$  and the backreaction (22). For  $\lambda_S = 10^{-4}$ , we set  $(N_{\text{DW}}, \ell, m, n) = (3, 2, 10, 6)$  in Fig. 1 and  $(N_{\text{DW}}, \ell, m, n) = (3, 2, 9, 6)$ ,  $(2, 3, 9, 6)$  in the left and right panels of Fig. 2, respectively. The value of  $N_{\text{DW}}$  and  $\ell$  are taken as prime number with each other,

which will be required for a bias solution to the axion domain wall problem. We note that the (mild) degeneracy of the orange lines for  $\ell = 2$  is attributed to the independence of  $m_{\text{PQ}}^2$  on  $v_{\text{PQ}}$ . In addition, it is possible to take many other sets of  $(\ell, m, n)$ . Since larger  $\ell$  and  $m$  give a more significant Planck suppression, the maximum value of  $\ell$  depends on  $m$  by assuming not too large  $|\lambda|$ . Let us enumerate possible parameter sets as follows:

$$\begin{aligned} (\ell, m, n) \ni & (1, 10, 6), (2, 10, 6) \\ & (1, 9, 6), (2, 9, 6), (3, 9, 6) \\ & (1, 8, 6), (2, 8, 6), (3, 8, 6), (4, 8, 6) \\ & (1, 7, 6), (2, 7, 6), (3, 7, 6), (4, 7, 6), (5, 7, 6). \end{aligned}$$

One can see that we need a very small value of  $|\lambda|$  unless we consider the maximum value of  $\ell$  for some  $m$  (e.g. see the left panel of Fig. 2), and such a small value of  $|\lambda|$  should be addressed in a UV model, which will be discussed in Sec. VI. Furthermore, one can see from Fig. 1 and Fig. 2 that these constraints put an upper bound on  $f_a$  (typically we find  $f_a \lesssim 10^{10}$  GeV for  $m \leq 2n-2$ ). The backreaction becomes more effective for larger  $f_a$ , while the condition  $T_{\text{osc}} > T_{\text{osc}}^{(\text{conv})}$  mildly depends on  $f_a$ .

In ref. [9], the region with non-negligible backreaction was not explicitly presented. In the next subsection, we will clarify what the backreaction is and its several phenomenological aspects by following the full equations of motion in the system.

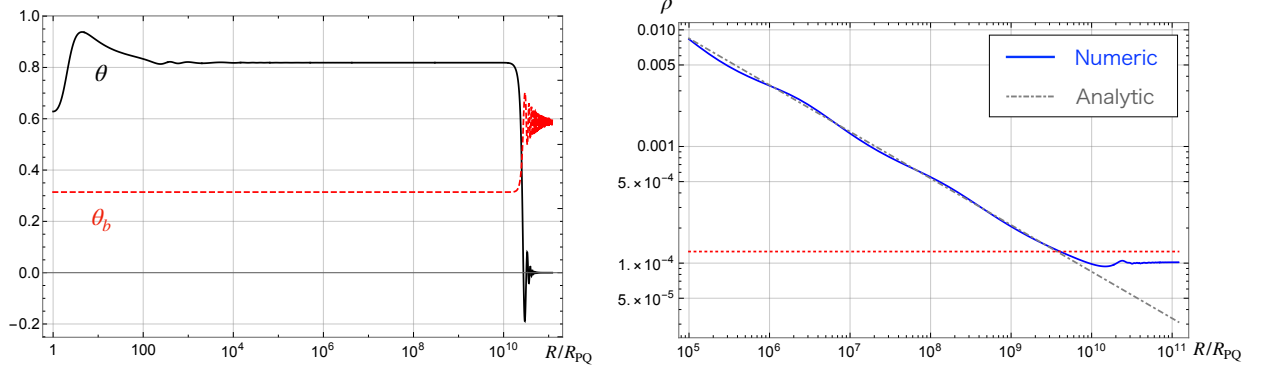


FIG. 3. Evolution of fields,  $\theta$ ,  $\theta_b$ , and  $\rho$  as a function of the scale factor. While the black solid and red dashed lines in the left panel represent the evolution of  $\theta$  and  $\theta_b$ , the blue line in the right panel does that of  $\rho$  with the scaling solution (9) denoted by the gray dot-dashed line. Here we set  $f_a = 10^{10}$  GeV,  $(N_{\text{DW}}, \ell, m, n) = (2, 3, 9, 6)$ ,  $|\lambda| = 0.5$ ,  $\lambda_S = 10^{-4}$ ,  $m_S = 10^{-20}$  GeV, and  $\delta = 1$  for the initial conditions,  $\theta_{\text{ini}} = \pi/5$ ,  $\theta_{b,\text{ini}} = \pi/10$ ,  $\chi_{\text{ini}}$  given by Eq. (9).

### C. Dynamics of the full system

Here let us discuss the dynamics of the full system to study the backreaction. We note that the radial component of  $P$  no longer affects the dynamics, as we assume that the Mexican-hat potential (the first term in Eq. (1)) is dominant. In the basis (12), the Lagrangian is given by

$$\mathcal{L} = \frac{1}{2}(\partial_\mu a)^2 + \frac{1}{2}(\partial_\mu \chi)^2 + \frac{1}{2}\chi^2(\partial_\mu \theta_b)^2 - V_{\text{PQ}}. \quad (23)$$

Hereafter, let us define dimensionless fields as

$$\theta \equiv \frac{a}{v_{\text{PQ}}}, \quad \theta_b \equiv \frac{b}{\chi}, \quad \rho \equiv \frac{\chi}{\bar{\chi}}, \quad (24)$$

with a normalization factor,

$$\bar{\chi} = \left[ \frac{2^{(m+\ell)/2-1} m! \ell! M_{\text{Pl}}^{m+\ell-4} H_{\text{PQ}}^2}{|\lambda| v_{\text{PQ}}^{\ell-2}} \right]^{1/m}, \quad (25)$$

where  $H_{\text{PQ}}$  is the Hubble parameter at  $T = v_{\text{PQ}}$ . Then we obtain the equations of motion,

$$\ddot{\theta} + 3H\dot{\theta} + \ell H_{\text{PQ}}^2 \rho^m \sin(\ell\theta + m\theta_b + \delta) + \frac{m_a^2 f_a}{v_{\text{PQ}}} \sin(N_{\text{DW}}\theta) = 0, \quad (26)$$

$$\ddot{\theta}_b + 3H\dot{\theta}_b + 2\frac{\dot{\rho}}{\rho}\dot{\theta}_b + \frac{m v_{\text{PQ}}^2 H_{\text{PQ}}^2}{\bar{\chi}^2} \rho^{m-2} \sin(\ell\theta + m\theta_b + \delta) = 0, \quad (27)$$

$$\ddot{\rho} + 3H\dot{\rho} + \frac{n\lambda_S^2}{2^{n-1}(n!)^2} \frac{\bar{\chi}^{2n-2}}{M_{\text{Pl}}^{2n-4}} \rho^{2n-1} - \dot{\theta}_b^2 \rho + m_S^2 \rho - \frac{m v_{\text{PQ}}^2 H_{\text{PQ}}^2}{\bar{\chi}^2} \rho^{m-1} \cos(\ell\theta + m\theta_b + \delta) = 0. \quad (28)$$

Fig. 3 shows the time evolution of the fields as a function of the scale factor  $R/R_{\text{PQ}}$  with  $R_{\text{PQ}}$  at  $T = v_{\text{PQ}}$ .

Here we set  $f_a = 10^{10}$  GeV,  $(N_{\text{DW}}, \ell, m, n) = (2, 3, 9, 6)$ ,  $|\lambda| = 0.5$  (which is beyond Eq. (22)),  $\lambda_S = 10^{-4}$ ,  $m_S = 10^{-20}$  GeV,  $\delta = 1$ , and assume constant numbers of effective degrees of freedom for energy density and entropy density,  $g_* = g_{*s} = 106.75$ . We take the initial conditions  $\theta_{\text{ini}} = \pi/5$ ,  $\theta_{b,\text{ini}} = \pi/10$ , and  $\chi_{\text{ini}}$  is taken in accordance with the scaling solution (9) at  $T = v_{\text{PQ}}$ . First, the axion motion is driven by  $V_{\text{PQ}}$ , but  $\theta_b$  still remains static. When the potential from the QCD effect becomes dominant over  $V_{\text{PQ}}$ , the axion oscillates around the minimum, inducing the small oscillation of  $\theta_b$ . The behavior of  $\rho$  looks very nontrivial and becomes constant when the backreaction cannot be neglected in the vicinity of the red dotted line derived from Eq. (21). This is because  $\theta$  and  $\theta_b$  move to the minimum of  $V_{\text{PQ}}$ , which makes the sign of the mixing term negative, and then the competition between  $|S|^{2n}$  and  $S^m P^\ell$  stabilizes a nonzero VEV of  $S$ . Since the vacuum structure is not altered by the evolution of phases or mass term  $m_S$ , this gives rise to a large deviation of the axion VEV from CP conserving points. Thus we must avoid such an inconsistent situation by considering the bound (22).

### IV. TOPOLOGICAL DEFECTS

At  $T \sim v_{\text{PQ}}$ ,  $P$  acquires a nonzero VEV, and the PQ symmetry is spontaneously broken. When it occurs after inflation, cosmic string appears. In our scenario where the axion starts to oscillate before the QCD crossover, domain walls are produced through the mixing-induced potential and connected with the cosmic strings, which is called the string-wall system. The number of domain walls attached with a cosmic string is given by  $\ell$ .

While the system is unstable for  $\ell = 1$ , it cannot collapse by itself for  $\ell > 1$  because the cosmic string is sustained by the tension of walls from multiple directions. Here, we discuss the evolution and the fate of the string-wall system for each case.

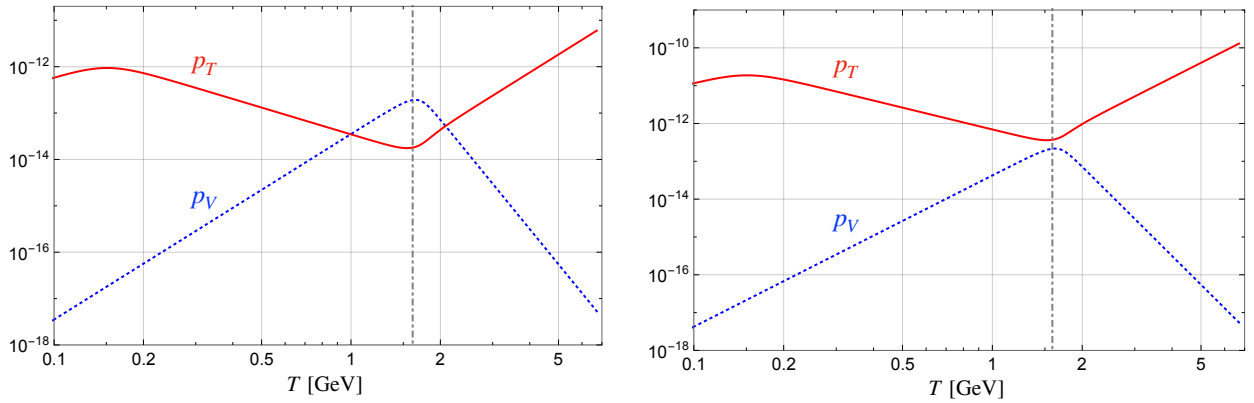


FIG. 4. The tension force (red solid) and volume pressure (blue dotted) in units of  $\text{GeV}^4$  as a function of temperature. We set  $(N_{\text{DW}}, \ell, m, n) = (3, 2, 10, 6)$ ,  $\lambda_S = 10^{-4}$ ,  $m_S = 10^{-20}$  GeV,  $f_a = 10^9$  GeV ( $2 \times 10^{10}$  GeV), and  $\lambda = \lambda^{(\text{max})} \simeq 0.01$  ( $3 \times 10^{-5}$ ) in the left (right) panel. The gray vertical line denotes the temperature  $T_{\text{tr}}$  (35).

### A. Short-lived system

First let us consider the case of  $\ell = 1$ , which was studied in ref. [9]. Since one domain wall is attached with each cosmic string, when the tension force acting on the domain wall is comparable to that on the string, the system becomes unstable. Given the wall and string tensions at  $T \gg \Lambda_{\text{QCD}}$ ,

$$\sigma_{\text{wall}}(T) \simeq \frac{8}{\ell^2} m_{\mathcal{PQ}}(T) v_{\text{PQ}}^2, \quad (29)$$

$$\mu_{\text{string}}(T) \simeq 2\pi v_{\text{PQ}}^2 \ln \left( \frac{v_{\text{PQ}}}{H(T)} \right), \quad (30)$$

we can estimate the condition that the system is broken as [9]

$$\frac{\sigma_{\text{wall}} H}{\mu_{\text{string}} H^2} \gtrsim 1 \quad (31)$$

$$\leftrightarrow m_{\mathcal{PQ}}(T) \gtrsim \frac{\pi \ell^2}{4} H(T) \ln \left( \frac{v_{\text{PQ}}}{H(T)} \right), \quad (32)$$

for  $T < T_{\text{osc}}$ . Naively, the condition is  $m_{\mathcal{PQ}} \gtrsim \mathcal{O}(10)H$ . Even if  $N_{\text{DW}} > 1$ , the string-wall system via the potential from QCD effects no longer forms, because the axion field at any spacial point settles into the single minimum of  $V_{\mathcal{PQ}}$ .

### B. Long-lived system

For  $\ell > 1$ , the string-wall system must be broken due to some destabilization effects. If the string-wall system is never broken or too long-lived, the domination of energy density or the overproduced axions would spoil the success of the standard cosmology, but once it collapses successfully, the axion DM can be produced with the correct abundance. From the perspective of the system made up by  $V_{\mathcal{PQ}}$ , the QCD potential seems to bias the symmetric

structure, as long as  $\ell$  and  $N_{\text{DW}}$  are co-prime number. However, we will find it nontrivial to conclude the fate of the system.

Let us begin with the discussion on the stability of the system in (semi)analytical way. There are two kinds of destabilization effects: one is a biased potential, the other is some structural instability. First, we focus on the biased potential.<sup>5</sup> A bias term against the string-wall system generates the volume pressure, which is estimated by the potential difference between two vacua,  $p_V \simeq \Delta V_{\text{bias}}$ . When the volume pressure becomes comparable to the tension force  $p_T$ , the system starts to be destabilized. In our case, while  $V_{\text{bias}} = V_{\text{QCD}}$  at  $T \gg \Lambda_{\text{QCD}}$ ,  $V_{\text{bias}} = V_{\mathcal{PQ}}$  at  $T \ll \Lambda_{\text{QCD}}$ , and the domain wall number can change from  $\ell$  to  $N_{\text{DW}}$ . To validate the system collapse in this complicated setup, we can numerically estimate  $p_V$  and  $p_T$ . The tension force is given by

$$p_T \simeq 4H \int_{\theta_{\text{min}1}}^{\theta_{\text{min}2}} d\theta \frac{|V(\theta)|}{\sqrt{m_{\mathcal{PQ}}^2 + m_a^2}}, \quad (33)$$

where  $V = V_{\mathcal{PQ}} + V_{\text{QCD}}$ , and  $\theta_{\text{min}1}, \theta_{\text{min}2} (> \theta_{\text{min}1})$  are the adjacent local minima of  $V_{\mathcal{PQ}}$ . The prefactor is chosen, so that  $p_T \sim 2\sigma_{\text{wall}}H$  in the high temperature limit. Fig. 4 describes the temperature dependence of the tension force  $p_T$  (red solid) and the volume pressure  $p_V$  (blue dotted) for  $(N_{\text{DW}}, \ell, m, n) = (3, 2, 10, 6)$ ,  $\lambda_S = 10^{-4}$ ,  $m_S = 10^{-20}$  GeV,  $f_a = 10^9$  GeV ( $2 \times 10^{10}$  GeV), and  $\lambda = \lambda^{(\text{max})} \simeq 0.01$  ( $3 \times 10^{-5}$ ) in the left (right) panel. We take the maximum value of  $\lambda$  to satisfy the backreaction constraint. The vertical gray line is estimated by

<sup>5</sup> Although both effects should be taken into account simultaneously, we take a limit that either effect is dominant in the following discussion.



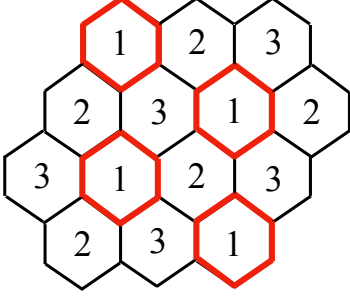


FIG. 5. Approximate description of the system for  $\ell = 3$  and  $N_{\text{DW}} = 2$  (a 2D slice perpendicular to the strings is shown). After  $V_{\text{QCD}}$  becomes dominant, the vacua numbered by 2 and 3 are integrated, and one vacuum is isolated. The black lines denote the initial domain walls, while the red lines the final domain walls.

$|V_{\text{QCD}}| \sim |V_{\text{PQ}}|$ , or

$$m_{\text{PQ}}(T_{\text{tr}}) \sim \frac{\ell}{N_{\text{DW}}} m_a(T_{\text{tr}}) \quad (34)$$

$$\leftrightarrow T_{\text{tr}} \simeq 1.6 \text{ GeV} \left( \frac{|\lambda|}{0.01} \right)^{-\alpha} \left( \frac{v_{\text{PQ}}}{2 \times 10^9 \text{ GeV}} \right)^{-\ell\alpha}, \quad (35)$$

where  $\alpha \equiv (2\tilde{b} + 2m/(n-1))^{-1}$ . At the boundary  $T = T_{\text{tr}}$ , the role of each potential is switched from bias to tension or vice versa. Assuming that it takes  $\Delta T \sim \mathcal{O}(1)$  GeV conservatively for the system to collapse completely, we find that  $f_a \lesssim 10^9$  GeV is required, as shown in the left panel of Fig. 4. This assumption is naively justified by the results of simulations [28].

Even for  $f_a \gtrsim 10^9$  GeV, the system is able to be destabilized by the structural instability. The mixing-induced potential makes the initial distribution of the axion field non-uniform. When the axion starts to oscillate by  $V_{\text{PQ}}$ , the axion field configuration is given by the domain wall solution, which is highly inhomogeneous in space. When  $V_{\text{QCD}}$  is turned on, the local minima of the potential are deformed and a new structure combining domain walls and strings appears around  $T \simeq T_{\text{tr}}$ , but in some case, the system cannot be stabilized in a symmetric way, as long as we consider  $\ell$  and  $N_{\text{DW}}$  which are co-prime numbers. Consider  $\ell > N_{\text{DW}}$ , e.g.,  $\ell = 3$ ,  $N_{\text{DW}} = 2$  (see Fig. 5). Initially, three domain walls are attached to one string in the most symmetric way. After  $V_{\text{QCD}}$  becomes dominant, one vacuum disappears and the vacuum structure is decomposed into the remaining two vacua. Due to the initial configuration, we can expect that one of them is isolated and collapses by the tension.

It should be noted that the system may not be destabilized by an asymmetric structure for  $m \geq 2n - 1$ . Since  $m_{\text{PQ}}$  decreases faster than  $H$  and becomes smaller than  $H$  at some temperature, the axion configuration can be rearranged by the gradient term. For a larger value of  $\lambda$ , the re-randomization might be mild, but we conservatively focus on  $m \leq 2n - 2$  in the following discussion.

So far, we have qualitatively discussed the destabilization of the system only in one specific case. However, it is unclear for different combinations of  $(\ell, N_{\text{DW}})$ , which will be discussed in Sec. VII. In short, to destabilize the system conservatively requires the following conditions:

$$f_a \lesssim 10^9 \text{ GeV}, \quad \text{for } \forall (\ell, N_{\text{DW}}), \quad (36)$$

or

$$(\ell, N_{\text{DW}}) = (3, 2), \quad \text{for } \forall f_a \text{ and } m \leq 2n - 2. \quad (37)$$

Note that  $\forall$  means all possible combinations or values of  $f_a$  which are restricted by the backreaction constraints. Moreover, there remain curious questions for the latter case, how much time it takes to collapse or how the dynamics depends on the size of  $V_{\text{PQ}}$ . To answer those questions requires a detailed simulation, which is left for a future study. Here we simply assume that the annihilation occurs after the potential minima are deformed, i.e. at  $T_{\text{ann}} = \kappa T_{\text{tr}}$ , with  $\kappa < 1$  a numerical parameter. Since the hexagons can shrink with the shape kept, the typical time scale is  $H^{-1}$ , or  $\kappa \sim \mathcal{O}(0.1)$  can be taken. The latter case is severer for the domain wall problem, and we focus on this case below.

Let us now estimate the abundance of the axion produced from the domain wall annihilation. Since the energy density of strings is diluted faster than that of domain walls, we here ignore the dynamics of strings. The evolution of energy densities of domain walls, axions, and gravitational waves are respectively given by

$$\frac{d\rho_{\text{wall}}}{dt} = -(1+p)H\rho_{\text{wall}} - \frac{d\rho_{\text{wall}}}{dt} \Big|_{\text{emission}}, \quad (38)$$

$$\frac{d\rho_a}{dt} = -3H\rho_a + \frac{d\rho_{w \rightarrow a}}{dt}, \quad (39)$$

$$\frac{d\rho_{\text{gw}}}{dt} = -(4+2p)H\rho_{\text{gw}} + \frac{d\rho_{w \rightarrow \text{gw}}}{dt}, \quad (40)$$

where  $p = m/(n-1)$ , and we assume that the total amount of the decay products from the domain wall consists of the axion and gravitational waves,

$$\frac{d\rho_{\text{wall}}}{dt} \Big|_{\text{emission}} = \frac{d\rho_{w \rightarrow a}}{dt} + \frac{d\rho_{w \rightarrow \text{gw}}}{dt}. \quad (41)$$

We assume the system follows the scaling law, and the domain wall tension is temperature dependent, or  $\rho_{\text{wall}} \propto H^{m/2(n-1)+1} \propto R^{-m/(n-1)-2}$ . In the scaling regime, the energy density of gravitational waves is given by  $\rho_{\text{gw}} \simeq \epsilon_{\text{gw}} G \sigma_{\text{wall}}^2$ , where  $\epsilon_{\text{gw}}$  is the efficiency of production. The dilution by the scaling law is compensated by the second terms in Eqs. (38), (40). We then obtain the rate of the axion production,

$$\frac{d\rho_{w \rightarrow a}}{dt} \simeq \frac{\sigma_{\text{wall}}}{2t^2} - 2\epsilon_{\text{gw}} \frac{G \sigma_{\text{wall}}^2}{t}. \quad (42)$$

As the potential from the QCD effects grows up, the tension force or the energy density of the system evolves as



shown in Fig. 4. Assuming that the produced axion has energy  $\sqrt{1 + \epsilon_a^2} m_a$  where  $\epsilon_a$  is defined as the momentum of the produced axion in units of  $m_a$ , the comoving number density of the axion is given by

$$\begin{aligned} N_{a,\text{dec}}(t) &\equiv R^3(t) n_{a,\text{dec}}(T) \\ &\simeq \int_{t_{\text{osc}}}^t dt' \frac{R^3(t')}{\sqrt{1 + \epsilon_a^2} m_a(t')} \frac{d\rho_{w \rightarrow a}}{dt'} \\ &\simeq \frac{R^3(t)}{\sqrt{1 + \epsilon_a^2} m_a(t)} \left[ \frac{\sigma_{\text{wall}}}{t} - \frac{4}{3-p} \epsilon_{\text{gw}} G \sigma_{\text{wall}}^2(t) \right]. \end{aligned} \quad (43)$$

Here  $n_{a,\text{dec}}$  denotes the number density of the produced axion, and we have used  $t \gg t_{\text{osc}}$  in the third equality. We can assume  $\sigma_{\text{wall}} \simeq 8 m_a f_a^2$ . In addition, the string decay also produces the axion from  $T \simeq v_{\text{PQ}}$  to  $T = T_{\text{osc}}$ . Since we focus on  $T_{\text{osc}} \gg T_{\text{osc}}^{(\text{conv})}$ , the string decay stops at a very early epoch, leading to the only subdominant contribution.

By using Eq. (35) and Eq. (43), we obtain the abundance of the axion produced from the domain wall,

$$\begin{aligned} \Omega_{a,\text{dec}} h^2 &= \frac{m_{a,0} N_{a,\text{dec}}(t_{\text{ann}})}{\rho_{\text{crit}} h^{-2} R_0^3} \\ &\simeq 0.12 \frac{1}{\sqrt{1 + \epsilon_a^2}} \left( \frac{\kappa}{0.1} \right)^{-1} \left( \frac{|\lambda|}{2 \times 10^{-4}} \right)^\alpha \\ &\times \left( \frac{N_{\text{DW}}}{2} \right)^{\ell\alpha} \left( \frac{f_a}{2.4 \times 10^{10} \text{ GeV}} \right)^{1+\ell\alpha}, \end{aligned} \quad (44)$$

where we set  $(\ell, m, n) = (3, 9, 6)$  and  $\lambda_S = 10^{-4}$ , and the contribution of gravitational waves is negligibly small. Since the annihilation temperature can be lower than that used in the estimation and  $N_{a,\text{dec}} \propto T_{\text{ann}}^{-1}$ , we note that the abundance can be enhanced, so that the upper bound on  $f_a$  would be severer. Although a smaller  $m$  can be also taken, the upper bound on  $f_a$  from the backreaction and  $T_{\text{osc}} > T_{\text{osc}}^{(\text{conv})}$  become tighter. Thus the domain wall problem is solved, as long as it is solved for  $(\ell, m, n) = (3, 9, 6)$ .

## V. AXION DM FROM MISALIGNMENT

We here consider the production of the axion DM via the (trapped) misalignment mechanism. The isocurvature perturbation constraint is also discussed. Finally, we find the total axion DM abundance from the domain wall decay and the misalignment mechanism, and clarify the viable parameter space to address the domain wall problem.

### A. Axion field dynamics

In addition to topological defects, coherent oscillations of the axion field contribute to the DM abundance via

the misalignment mechanism [6–8]. The extra potential induced by the mixing term makes the axion evolution more nontrivial, which can be classified into the so-called trapped misalignment [10–18]. The dynamics is classified into two regimes [16]:

$$\begin{aligned} \text{(I)} \quad & |\theta_{\text{min}}^{(\text{PQ})} - \theta_{\text{min}}^{(\text{QCD})}| \ll \frac{\pi}{\ell} \quad (\text{smooth shift regime}), \\ \text{(II)} \quad & |\theta_{\text{min}}^{(\text{PQ})} - \theta_{\text{min}}^{(\text{QCD})}| \gtrsim \frac{\pi}{\ell} \quad (\text{trapped regime}). \end{aligned}$$

Here we define  $\theta_{\text{min}}^{(\text{PQ})} \equiv (2\pi k - \delta')/\ell$  as the minimum of  $V_{\text{PQ}}$  at which the axion first oscillates, with  $\delta' \equiv \delta + m\theta_b$  (which can be identified as a free parameter) and  $k \in \mathbb{Z}$ , and  $\theta_{\text{min}}^{(\text{QCD})}$  is taken as the closest minimum of  $V_{\text{QCD}}$  to it. In the smooth shift regime, if the trapping effect of the extra potential is strong enough, any additional oscillation is not induced when the potential minimum shifts due to  $V_{\text{QCD}}$ . This means that the axion follows the shift of the potential minimum, and the suppression occurs when  $|\dot{m}_{\text{eff}}/m_{\text{eff}}^2| \ll 1$  where  $m_{\text{eff}} \equiv \sqrt{|V''(a)|}$  evaluated at the temporal minimum [13]. This is called the adiabatic suppression mechanism [29] ([10, 12, 13] for the QCD axion). In the trapped regime, the axion is trapped at the wrong vacuum for a longer time, and after the wrong vacuum vanishes, the axion starts to oscillate again around the CP conserving minimum.

To recognize the two regimes, we show the time evolution of the axion field and the kinetic energy normalized by  $s \cdot m_a$  ( $s$  is the entropy density) as a function of  $T_{\text{osc}}^{(\text{conv})}/T$  in Fig. 6. Since the potential energy contribution to the number density is not conserved because  $m_{\text{PQ}}$  is time-dependent, we plot the kinetic energy, as will be addressed later. Here we choose an example parameter set  $f_a = 10^{10} \text{ GeV}$ ,  $(N_{\text{DW}}, \ell, m, n) = (2, 3, 9, 6)$ ,  $|\lambda| = 3 \times 10^{-3}$ ,  $\lambda_S = 10^{-4}$ ,  $\delta' = \pi/4$ , and use the temperature-dependent  $g_*$  and  $g_{*s}$  estimated in ref. [30]. The value of  $|\lambda|$  corresponds to the maximum value (22) for  $m_S \sim 10^{-20} \text{ GeV}$ . The red solid and blue dotted lines represent the evolutions for the smooth shift regime and the trapped regime, respectively. The initial conditions are chosen, so that the initial oscillation amplitude is set to  $|\theta_{\text{ini}} - \theta_{\text{min}}^{(\text{PQ})}| = \pi/6$ . One can see that the kinetic energy in the case (I) is much smaller than that in the case (II). This is not mainly because the (second) oscillation amplitude is small, but because of the adiabatic suppression. Even for the case (I), however, the oscillation is not strongly suppressed, because the backreaction constraint put the upper bound on  $|\lambda|$  (22) and the trapping effect cannot be very strong in our model. Thus, a numerical estimate of the abundance is required for considering such a weak but non-negligible trapping effect.

### B. Abundance

In the post-inflationary scenario, the abundance of the axion DM can be estimated as the average of contribu-

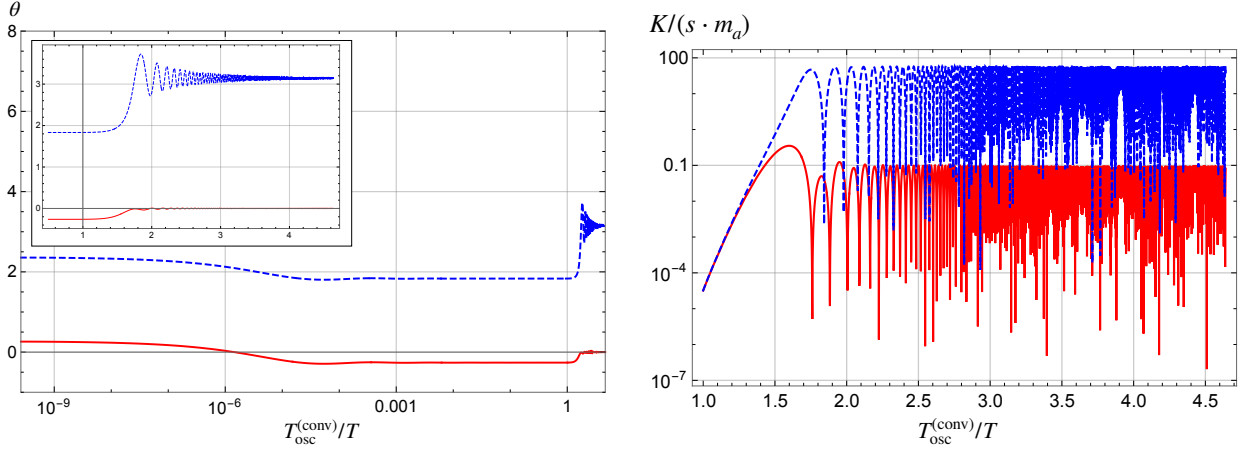


FIG. 6. Evolution of the axion field (left) and the kinetic energy (right) as a function of  $T_{\text{osc}}^{(\text{conv})}/T$ . The region of  $T_{\text{osc}}^{(\text{conv})}/T = \mathcal{O}(1)$  is enlarged in the window inside the left panel. We set  $f_a = 10^{10}$  GeV,  $(N_{\text{DW}}, \ell, m, n) = (2, 3, 9, 6)$ ,  $|\lambda| = 3 \times 10^{-3}$ ,  $\lambda_S = 10^{-4}$ , and  $\delta' = \pi/4$ . The red solid and blue dotted lines represent the evolution for the smooth shift regime and the trapped regime, respectively. The initial oscillation amplitude of the axion field is taken to be  $\pi/6$ .

tions from all possible initial values of the axion field. The number density is given by

$$n_a \simeq \frac{1}{2\pi} \int_{-\pi}^{\pi} d\theta_{\text{ini}} n_a(\theta_{\text{ini}}), \quad (45)$$

where  $n_a(\theta_{\text{ini}})$  represents the number density for an initial value of the axion field  $\theta_{\text{ini}}$ .

To perform a numerical estimation, we use several approximations. First, we assume that when the axion field oscillates around a common minimum  $\theta_{\text{min}}^{(\mathcal{PQ})}$ , the abundance does not depend on  $\theta_{\text{ini}}$ . In fact, this assumption is justified unless  $V_{\mathcal{PQ}}$  aligns with  $V_{\text{QCD}}$ , i.e.  $|\theta_{\text{min}}^{(\mathcal{PQ})} - \theta_{\text{max}}^{(\text{QCD})}| \ll 1$ . One can find it plausible from the left panel of Fig. 6 where the axion has only a negligibly small oscillation amplitude around the minimum of  $V_{\mathcal{PQ}}$ . When the alignment occurs in the potentials, strong dependence on  $\theta_{\text{ini}}$  appears due to the anharmonic effect.<sup>6</sup> As the second approximation, we use the formula (9) for the scaling solution without following the full system. Thirdly, the energy density is estimated as the time average of the kinetic energy,

$$\begin{aligned} \rho_a &= \frac{\dot{a}^2}{2} + V_{\text{QCD}} + V_{\mathcal{PQ}} \\ &\simeq 2 \frac{1}{\delta t} \int_{\delta t} dt \frac{\dot{a}^2}{2}, \end{aligned} \quad (46)$$

after the kinetic energy amplitude normalized by the entropy density becomes constant. Here  $\delta t$  is taken to be much larger than  $m_a^{-1}$ . Since the spectator field has a

large amplitude until it oscillates when  $m_S \sim H$ , the axion has a non-negligible, time-dependent vacuum energy. To estimate the current abundance, we would need to analyze the full equations of motion at least just after  $m_S \sim H$ . However, since the amplitude of the kinetic energy becomes constant after the oscillation around  $V_{\text{QCD}}$ , which is finally expected to be comparable to the potential energy, it is sufficient to follow the axion equation of motion only until the oscillation around  $V_{\text{QCD}}$ , reducing the computation time.

We can have two types of estimation: (A)  $\ell < N_{\text{DW}}$  and (B)  $\ell > N_{\text{DW}}$ .<sup>7</sup> In the following estimation, we focus on  $m = 9$  ( $= 2n - 3$ ) case, but we numerically confirmed that the overall behavior is the same as the case of  $m = 10$  ( $= 2n - 2$ ).

### 1. Case (A)

In this case, there is no trapped regime, and the abundance can be basically suppressed by the adiabatic suppression mechanism. Assuming that the initial axion field is uniformly distributed, the number density of the axion is given by

$$n_a \simeq \frac{1}{\ell} \sum_{r=1}^{\ell} n_a^{(r)}. \quad (47)$$

Here  $n_a^{(r)} \equiv \rho_a^{(r)}/m_a$  is estimated for the case where the axion starts to oscillate around each  $\theta_{\text{min}}^{(\mathcal{PQ})}$ .

<sup>6</sup> Actually, there is a  $\theta_{\text{ini}}$  dependence even not for the alignment case due to the anharmonic effect, but it appears only in a very tiny range of  $\theta_{\text{ini}}$  and can be integrated out approximately.

<sup>7</sup> As we mentioned in Sec. IV, it is unclear if the string-wall system can collapse except for  $(\ell, m, n) = (3, 9, 6)$ . However, we take several combinations in this section to show how the misalignment production is modified by the extra potential.

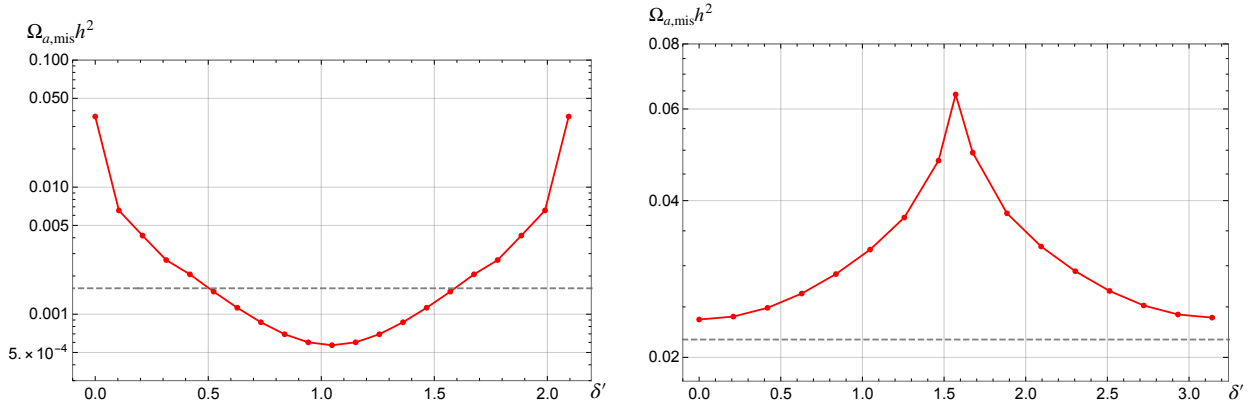


FIG. 7. The abundance produced via the misalignment mechanism as a function of  $\delta'$  for  $N_{\text{DW}} = 3, 2$  in the left and right panels, respectively. While the left panel shows the result for  $(\ell, m, n) = (2, 9, 6)$  and  $f_a = 10^{10}$  GeV, the right panel shows for  $(\ell, m, n) = (3, 9, 6)$  and  $f_a = 8 \times 10^{10}$  GeV. In both panels, we set  $|\lambda| = |\lambda^{(\text{max})}|$ . The gray dashed line denotes the abundance of the conventional QCD axion (48).

In the left panel of Fig. 7, we show the numerical result for  $(N_{\text{DW}}, \ell, m, n) = (3, 2, 9, 6)$  as a function of the relative phase  $\delta'$ . Here we choose an example parameter set,  $f_a = 10^{10}$  GeV,  $\lambda_S = 10^{-4}$ , and  $|\lambda| = |\lambda^{(\text{max})}|$ . The gray horizontal line denotes the conventional QCD axion abundance [31],

$$\Omega_{a,\text{mis}}^{(\text{conv})} h^2 \simeq 1.6 \times 10^{-3} \left( \frac{g_*}{80} \right)^{\frac{\tilde{b}+2}{2(\tilde{b}+4)}} \left( \frac{f_a}{10^{10} \text{ GeV}} \right)^{\frac{\tilde{b}+6}{\tilde{b}+4}}. \quad (48)$$

Here the anharmonic effect in terms of  $\theta_{\text{ini}}$  is taken into account. One can see that the abundance is suppressed via the adiabatic suppression mechanism. At  $\delta' = 2\pi j/3$  with  $j = 0, 1, 2, \dots$ , where  $V_{\text{PQ}}$  aligns with  $V_{\text{QCD}}$ , the abundance enhances because the adiabatic suppression mechanism no longer works due to the anharmonic effect [13]. Our approximation gets worse in this range, because the dependence on  $\theta_{\text{ini}}$  is no longer negligible. Requiring such a significant fine tuning does not motivate us to further explore this case.

## 2. Case (B)

For  $\ell > N_{\text{DW}}$ , there are  $(\ell - N_{\text{DW}})$  trapped regimes. Assuming the flat distribution of the initial axion field, we obtain the number density of the axion,

$$n_a \simeq \frac{\ell - N_{\text{DW}}}{\ell} n_a^{(\text{trapped})} + \frac{N_{\text{DW}}}{\ell} n_a^{(\text{smooth})}, \quad (49)$$

where  $n_a^{(\text{trapped})}$  and  $n_a^{(\text{smooth})}$  are the number densities for the trapped and smooth shift regimes, respectively. The first contribution is dominant according to the numerical results in Fig. 6.

In the right panel of Fig. 7, the numerical result of the abundance for  $(N_{\text{DW}}, \ell, m, n) = (2, 3, 9, 6)$  are shown for  $f_a = 8 \times 10^{10}$  GeV,  $\lambda_S = 10^{-4}$ , and  $|\lambda| = |\lambda^{(\text{max})}| \simeq 10^{-5}$ .

We can see that the abundance is enhanced compared to that of the conventional QCD axion. We note again that our approximation gets worse in the range of  $|\delta' - 2\pi(j + 1/4)| \ll 1$ .

## C. Isocurvature perturbations

Let us briefly discuss the isocurvature perturbations of the axion field. Although we assume that the PQ symmetry is spontaneously broken after inflation, the axion field has isocurvature fluctuations due to the mixing with the phase  $b$  of  $S$  which acquires quantum fluctuations during inflation [9]. The fluctuation of the phase  $b$  during inflation is given by

$$\delta b_{\text{inf}} \simeq \frac{H_{\text{inf}}}{2\pi}. \quad (50)$$

As  $S$  obeys the scaling solution, the fluctuation evolves with time,

$$\delta b \simeq \frac{\chi}{\langle \chi_{\text{inf}} \rangle} \delta b_{\text{inf}}. \quad (51)$$

Since  $\delta b$  induces the fluctuations of center of the oscillation, the fluctuation of the axion field is estimated as

$$\frac{\delta a}{f_a} \simeq \frac{m N_{\text{DW}}}{\ell} \frac{\delta b}{\chi} \simeq \frac{m N_{\text{DW}} H_{\text{inf}}}{2\pi \ell \langle \chi_{\text{inf}} \rangle}. \quad (52)$$

Assuming that the first oscillation induced by  $V_{\text{PQ}}$  does not contribute to the DM abundance, the dimensionless power spectrum is given by [32]

$$\Delta_{\text{iso}}^2 \equiv \frac{k^3}{2\pi} \mathcal{P}_{\text{iso}} \simeq \left( \frac{\Omega_{\text{mis}}}{\Omega_{\text{DM}}} \frac{\partial \Omega_{\text{mis}}}{\partial \ln \theta_{\text{amp}}} \frac{\delta a}{f_a} \right)^2, \quad (53)$$

where one can estimate the amplitude of oscillation as  $\theta_{\text{amp}} \sim |\theta_{\text{min}}^{(\text{PQ})} - \theta_{\text{min}}^{(\text{QCD})}|$ . The recent result of the Planck

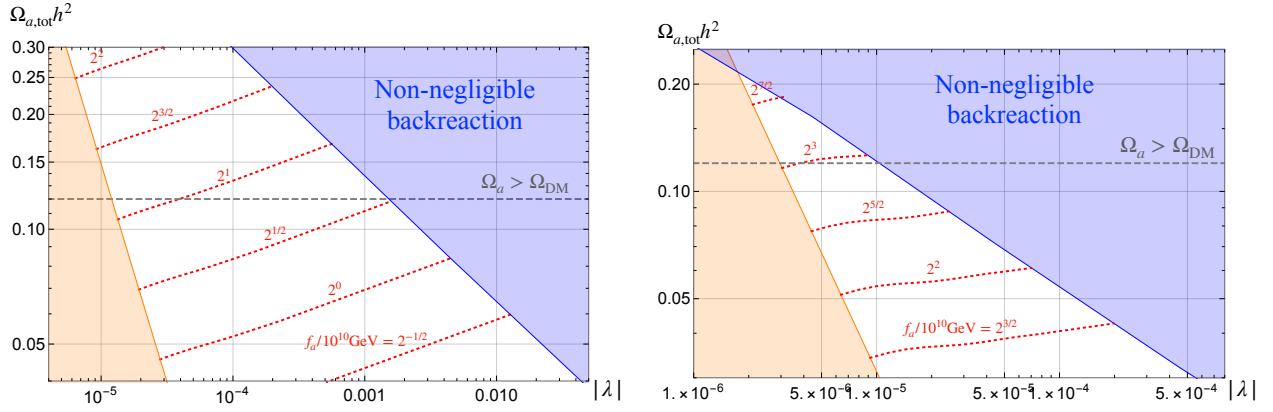


FIG. 8. The total axion abundance  $\Omega_{a,\text{tot}} h^2$  as a function of  $|\lambda|$  for  $\delta' = 1$ ,  $\lambda_S = 10^{-4}$ ,  $m_S = 10^{-20}$  GeV, and  $(N_{\text{DW}}, \ell, m, n) = (2, 3, 9, 6)$ . We take  $\kappa = 0.1, 0.5$  in the left and right panels, respectively. The blue and orange shaded regions are excluded by the constraints of the backreaction (22) and the stability of the string-wall system. The gray dashed line gives the correct DM abundance.

collaboration [33] puts an upper bound on the scale-invariant and uncorrelated isocurvature perturbation,

$$\beta_{\text{iso}}(k_0) \equiv \frac{\mathcal{P}_{\text{iso}}}{\mathcal{P}_\zeta} < 0.038, \quad (54)$$

$$\leftrightarrow \Delta_{\text{iso}}^2 < 8.3 \times 10^{-11}, \quad (55)$$

where  $\mathcal{P}_\zeta$  represents the power spectrum of the adiabatic perturbations.

Neglecting the anharmonic effect, the upper bound on the inflation scale is estimated as

$$H_{\text{inf}} \lesssim 2.5 \times 10^{15} \text{ GeV} \left( \sqrt{\frac{c_S}{n}} \frac{n!}{\lambda_S} \right)^{\frac{1}{n-2}} \times \left( \frac{\ell}{m N_{\text{DW}}} \right)^{\frac{n-1}{n-2}} \left( \frac{10^{-2}}{\Omega_{\text{mis}}/\Omega_{\text{DM}}} \right)^{\frac{n-1}{n-2}}. \quad (56)$$

For example,  $H_{\text{inf}} \lesssim 1.0 \times 10^{15}$  GeV for  $(N_{\text{DW}}, \ell, m, n) = (2, 3, 9, 6)$ ,  $\lambda_S = 1$ ,  $c_S = 1$ , and  $\Omega_{\text{mis}}/\Omega_{\text{DM}} = 10^{-2}$ . Considering the current bound on  $H_{\text{inf}}$ , we are able to take  $10^{-4} \lesssim \lambda_S \lesssim 1$ . Note that when  $\delta'$  is finely tuned to the value where the potentials align with each other, the isocurvature bound is significantly enhanced by the anharmonic effect, as can be seen from Fig. 7.

#### D. Total abundance

Including the contribution from the misalignment production, let us clarify the viable parameter space for solving the domain wall problem. The total abundance of the axion DM is given by the sum of Eq. (44) and Eq. (47) or Eq. (49), i.e.,

$$\Omega_{a,\text{tot}} \simeq \Omega_{a,\text{dec}} + \Omega_{a,\text{mis}}. \quad (57)$$

Fig. 8 describes the total axion abundance as a function of  $|\lambda|$  with the red dotted contours of  $f_a/(10^{10} \text{ GeV}) =$

$2^{-1/2} - 2^2$  ( $2^{3/2} - 2^{7/2}$ ) for  $\kappa = 0.1$  (0.5). While the blue shaded region is excluded by the constraint of the backreaction (22), the string-wall system cannot collapse because  $T_{\text{osc}} \lesssim T_{\text{osc}}^{(\text{conv})}$  in the orange shaded region. We set  $(N_{\text{DW}}, \ell, m, n) = (2, 3, 9, 6)$ ,  $\delta' = 1$ ,  $\lambda_S = 10^{-4}$ , and  $m_S = 10^{-20}$  GeV. The total abundance is strongly dependent on the annihilation temperature  $\kappa$ . For a given  $f_a$ , the maximum and minimum of  $|\lambda|$  are determined from the backreaction and the stability of the string-wall system. Although we need precise simulations,  $f_a \lesssim 8 \times 10^{10}$  GeV is required to avoid the overproduction of the axion for  $\kappa \gtrsim 0.5$ . However, if the string-wall system is very long-lived and  $\kappa \ll \mathcal{O}(0.1)$ , the upper bound on  $f_a$  would be severer. When  $\kappa$  is relatively large and the upper bound on  $f_a$  is large, the misalignment axion production gives a relevant contribution,  $\Omega_{a,\text{mis}}/\Omega_{a,\text{tot}} = \mathcal{O}(10)\%$ . Still, the isocurvature bound is given by  $H_{\text{inf}} \lesssim 10^{14}$  GeV.

## VI. UV MODELS

The scalar potential in Eq. (1) does not contain higher dimensional terms such as the terms with any lower powers of  $|S|$  and the  $S$ - $P$  mixing terms with other powers. To explain the specific potential form without fine tuning, we consider a supersymmetric version of the model. The SUSY model for  $\ell = 1$  has been discussed in ref. [9]. Our focus here is to explore models for  $\ell \geq 2$ . In particular, we consider the case of  $(\ell, m, n) = (2, 9, 6)$  as our benchmark.

Let us consider a superpotential that respects both the  $U(1)_{\text{R}}$  and  $U(1)_{\text{PQ}}$  symmetries,

$$W = X(P\bar{P} - v_{\text{PQ}}^2) + \frac{\lambda_S}{6!} \frac{Y S^6}{M_{\text{Pl}}^4} + \lambda Z \left( \frac{P^2}{2!} + \frac{S^9}{9! M_{\text{Pl}}^7} \right). \quad (58)$$

	$X$	$Y$	$Z$	$S$	$P$	$\bar{P}$
$U(1)_R$	2	2	2	0	0	0
$U(1)_{PQ}$	0	-12	-18	2	9	-9

TABLE I. Charge assignments of the chiral superfields under  $U(1)_{PQ}$  and  $U(1)_R$ .

Here,  $X$ ,  $P$ ,  $\bar{P}$ ,  $S$ ,  $Z$ , and  $Y$  are chiral superfields whose charges under the  $U(1)_R$  and  $U(1)_{PQ}$  are listed in Table I. The  $F$ -term components of  $X$ ,  $Y$ , and  $Z$  generate the scalar potential given in Eq. (1). The mass term for the scalar component of  $S$  arises from SUSY breaking effects. In addition to the terms shown above, higher dimensional terms in the superpotential such as

$$W \supset X(P\bar{P})^2, \quad XS^9\bar{P}^2, \quad YS^6P\bar{P}, \quad ZP^3\bar{P}, \quad (59)$$

may also appear. However, these terms do not generate lower powers of  $|S|$ , and they are sub-leading compared to the relevant  $S$ - $P$  mixing term. Moreover, higher dimensional operators in the Kähler potential, such as

$$K \sim \frac{1}{M_{Pl}^2}(|X|^2|S|^2 + |Y|^2|S|^2 + |S|^4), \quad (60)$$

do not induce lower dimensional terms for  $|S|^n$ , as discussed in ref. [9]. The smallness of the couplings  $\lambda_S$  and  $\lambda$  is 't Hooft natural because the phase rotation symmetries of  $Y$  and  $Z$  are enhanced in the limit of  $\lambda_S \rightarrow 0$  and  $\lambda \rightarrow 0$ . We can also explain the smallness by introducing some spontaneously broken symmetries as in the case of ref. [34]

The small mass of  $S$ , where typically we take it around  $m_S = 10^{-20}$  GeV, requires significant fine tuning. In supersymmetric models,  $m_S$  is generally given by the order of the gravitino mass,  $m_{3/2} \sim \Lambda^2/M_{Pl}$ , where  $\Lambda$  denotes the SUSY breaking scale. This mass scale is generated by the Kähler term of the form  $K \sim |T|^2|S|^2/M_{Pl}^2$  where  $T$  is the SUSY breaking field. While the gravitino mass can be much smaller than the soft masses of sfermions and gauginos, achieving  $m_S = 10^{-20}$  GeV still demands severe fine tuning. This problem can be addressed if the SUSY breaking sector is sequestered from the  $S$ - $P$  sector by e.g. using no-scale Kähler potential [35]. In this case, the scalar and fermionic superpartners of the axion, the *saxion* and *axino*, can be very light, and their impact on cosmology is a non-trivial issue, which is left for a future study.

Lastly, let us also mention models with other combinations of  $(\ell, m, n)$ , including the case  $(\ell, m, n) = (3, 9, 6)$ , which corresponds to the scenario illustrated in Fig. 5. Similar to Eq. (58), one can construct a superpotential that generates both the  $|S|^{2n}$  term and the mixing term between  $P$  and  $S$ . Such a superpotential generally respects the  $U(1)_{PQ}$  and  $U(1)_R$  symmetries. However, relatively lower dimensional operators of the form,

$$V \sim \frac{|S|^{2k_s}|\bar{P}|^{2k_p}}{M_{Pl}^{2k_s+2k_p-4}}, \quad (61)$$

with positive integers  $k_s, k_p$ , may also be allowed. These terms can be problematic for our scenario if  $S$  acquires a large VEV, as they can shift the minimum of the QCD axion potential. A detailed analysis of such generic setups will be performed elsewhere.

## VII. CONCLUSIONS AND DISCUSSIONS

We have explored the dynamics of a post-inflationary QCD axion coupled to a light scalar field, focusing on their interplay in resolving the domain wall problem and generating the axion DM. The spectator scalar field acquires a nonzero VEV during inflation, inducing an effective PQ-violating interaction that leads to an axion potential with multiple degenerate vacua below the PQ phase transition. This structure results in the formation of string-domain wall networks. At the QCD phase transition, a new potential contribution triggers the decay of domain walls before they dominate the Universe. As the spectator scalar field relaxes to its true minimum, the effective PQ violation is turned off, realigning the axion potential with the QCD vacuum. We have followed the evolution of the axion-scalar system and studied axion DM production via domain wall decay and misalignment. Notably, we find that in some cases, the string-wall network can decay due to structural instability rather than volume pressure, enabling successful DM production with a higher axion decay constant than in conventional scenarios, without fine-tuning.

We have discussed how the string-wall system is destabilized by the structural instability for  $(\ell, N_{DW}) = (3, 2)$  in the presence of the extra potential  $V_{PQ}$ . Here we explore the other cases of  $(\ell, N_{DW})$ . For example, consider  $(\ell, N_{DW}) = (4, 3)$ . The initial network looks like lattice denoted by the black solid lines in the left panel of Fig. 9. At the QCD scale, one wall disappears and the ladder-like structure remains (red solid lines). Although it looks unstable in the direction perpendicular to the ladder, one can see from the overall structure that it may be stable or very long-lived. For  $\ell < N_{DW}$ , e.g.,  $\ell = 2, N_{DW} = 5$ , the initial configuration is given by a sequential structure of one string attached by two domain walls, shown in the right panel of Fig. 9. Considering the scaling law, we expect that the original two domain walls are likely to be decomposed into two or three domain walls after  $V_{QCD}$  becomes dominant. Since the part formed by three domain walls has stronger tension force, it shrinks so that the string and anti-string are pair-annihilated. Still, it seems that a chain-like defect made up by two domain walls without strings remains stable. Although we conclude that the system is naively stable except for  $(\ell, N_{DW}) = (3, 2)$  and  $f_a \lesssim 10^9$  GeV, the fate is still unclear and should be clarified by simulations. Lastly, let us comment on another destabilization mechanism, where if the initial population of the axion field is biased, the structure can collapse immediately [36–45]. In most literature,  $N_{DW} = 2$  case was studied because the percolation

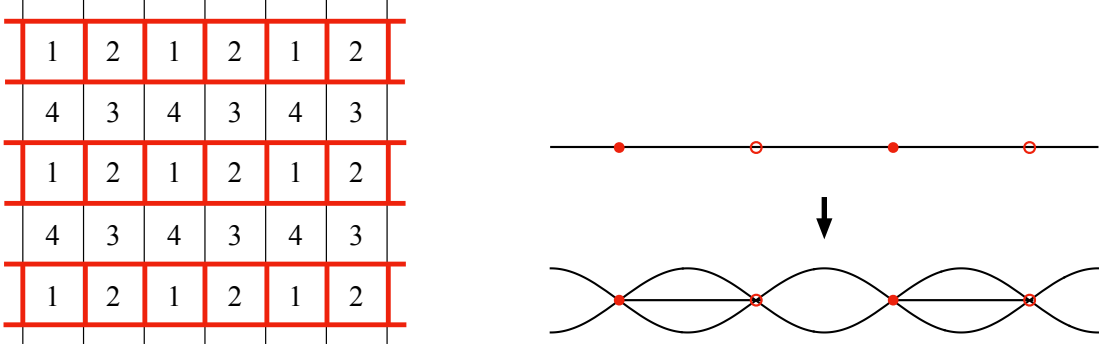


FIG. 9. Left: the system for  $\ell = 4$ ,  $N_{\text{DW}} = 3$ . The red solid lines represent the structure above the QCD scale. Right: the system for  $\ell = 2$ ,  $N_{\text{DW}} = 5$ . The red bullets and circles denote the strings and anti-strings, and the black line is the domain wall.

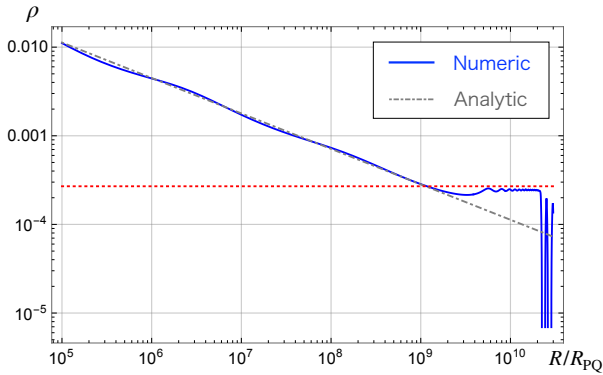


FIG. 10. The time evolution of the real spectator field for  $(N_{\text{DW}}, \ell, m, n) = (1, 2, 9, 6)$ . We set  $|\lambda| = 10^{-8}$  and  $\lambda_S = 10^{-4}$ ,  $m_S = 10^{-20}$  GeV,  $f_a = 10^{10}$  GeV, and  $\delta = -\pi/5$ . The red dotted line corresponds to Eq. (21). The oscillation begins at the QCD scale,  $T \simeq v_{\text{PQ}} \cdot (R_{\text{PQ}}/R) \sim \Lambda_{\text{QCD}}$ .

theory works. If we identify the string-wall system created by the extra potential as the initial population, the stability of the system can be discussed. Although there are several unclear points, e.g. how the case of  $N_{\text{DW}} \neq 2$  is investigated in a percolation theory-like way, it may be an interesting direction for a future study.

In Sec. III C, we have followed the full equations of motion to reveal the backreaction and found it unavoidable. Nevertheless, let us mention one possible and interesting way out to consider a large mixing interaction. The reason why  $S$  never oscillates is that the sign of the mixing term is necessarily negative. One potential way to flip the sign is to consider a real spectator field or to replace the mixing term  $S^m P^\ell$  with  $|S|^m P^\ell$ . In this case, the cosine term in the mixing term changes from negative to positive when the axion starts to oscillate by  $V_{\text{QCD}}$ , i.e.  $\cos(\ell\theta_{\min}^{(\text{PQ})} + \delta) \rightarrow \cos\delta$  with  $|\delta| < \pi/2$ , as long as  $N_{\text{DW}}$  is equal to 1 or a number which is not prime with  $\ell$ . In Fig. 10, we show the time evolution of  $S$  for  $(N_{\text{DW}}, \ell, m, n) = (1, 2, 9, 6)$  and  $|\lambda| = 10^{-8}$  which is over the bound (22), and one can find that  $S$  oscillates at the

QCD scale. For a large  $\lambda$ , the trapped misalignment is more remarkable, and the abundance is significantly enhanced. The estimation of the abundance was made in ref. [16], and we can expect that there is an upper bound on  $|\lambda|$ , because the abundance becomes independent of  $f_a$  and increases with the strength of the trapping effect. In addition, the oscillation amplitude of  $S$  is larger for larger  $|\lambda|$ , and the oscillation energy would be dominant. If we introduce a coupling of  $S$  with light fermions to make  $S$  decay into them, the energy remains as dark radiation, leading to another upper bound on  $|\lambda|$ .

Let us discuss the effect of the mixing term on the neutron EDM. When the Hubble parameter becomes comparable to  $m_S$ , the spectator field starts to oscillate around the origin. The current oscillation amplitude is estimated by

$$\frac{|S(T_0)|}{f_a} \simeq \sqrt{\frac{s_0}{s_{S_{\text{osc}}}}} \frac{|S(T_{S_{\text{osc}}})|}{f_a} \simeq 10^{-16} \left( \frac{10^{10} \text{ GeV}}{f_a} \right) \quad (62)$$

where  $T_{S_{\text{osc}}}$  denotes the temperature that  $S$  starts to oscillate,  $s_0, s_{S_{\text{osc}}}$  are the entropy densities estimated at  $T = T_0, T_{S_{\text{osc}}}$ , respectively, and we set  $m_S = 10^{-20}$  GeV and  $(\ell, m, n) = (2, 9, 6)$ . This induces the deviation from the CP conserving minimum,  $\delta\theta_{\min} \simeq 10^{-175}$ , which is negligibly tiny compared to the current bound on the static EDM. In this class of models, the axion minimum at present can oscillate due to the much longer timescale of  $S$ 's oscillation compared to that of the axion. While the amplitude of  $S$  may be too small for the effect to be observable, the time-dependent EDM nevertheless presents an intriguing possibility in principle [46].

## ACKNOWLEDGMENTS

We would like to thank Qianshu Lu and Yu-Cheng Qiu for fruitful discussions. Y.N. is supported by Natural Science Foundation of Shanghai. M.S. is supported by the MUR projects 2017L5W2PT. M.S. also acknowledges the European Union - NextGenerationEU, in the framework

- 
- [1] C. A. Baker *et al.*, Phys. Rev. Lett. **97**, 131801 (2006), arXiv:hep-ex/0602020.
- [2] J. M. Pendlebury *et al.*, Phys. Rev. D **92**, 092003 (2015), arXiv:1509.04411 [hep-ex].
- [3] R. D. Peccei and H. R. Quinn, Phys. Rev. Lett. **38**, 1440 (1977).
- [4] S. Weinberg, Phys. Rev. Lett. **40**, 223 (1978).
- [5] F. Wilczek, Phys. Rev. Lett. **40**, 279 (1978).
- [6] J. Preskill, M. B. Wise, and F. Wilczek, Phys. Lett. B **120**, 127 (1983).
- [7] L. F. Abbott and P. Sikivie, Phys. Lett. B **120**, 133 (1983).
- [8] M. Dine and W. Fischler, Phys. Lett. B **120**, 137 (1983).
- [9] M. Ibe, S. Kobayashi, M. Suzuki, and T. T. Yanagida, Phys. Rev. D **101**, 035029 (2020), arXiv:1909.01604 [hep-ph].
- [10] M. Kawasaki, F. Takahashi, and M. Yamada, Phys. Lett. B **753**, 677 (2016), arXiv:1511.05030 [hep-ph].
- [11] T. Higaki, K. S. Jeong, N. Kitajima, and F. Takahashi, JHEP **06**, 150 (2016), arXiv:1603.02090 [hep-ph].
- [12] M. Kawasaki, F. Takahashi, and M. Yamada, JHEP **01**, 053 (2018), arXiv:1708.06047 [hep-ph].
- [13] S. Nakagawa, F. Takahashi, and M. Yamada, JCAP **05**, 062 (2021), arXiv:2012.13592 [hep-ph].
- [14] L. Di Luzio, B. Gavela, P. Quilez, and A. Ringwald, JHEP **05**, 184 (2021), arXiv:2102.00012 [hep-ph].
- [15] L. Di Luzio, B. Gavela, P. Quilez, and A. Ringwald, JCAP **10**, 001 (2021), arXiv:2102.01082 [hep-ph].
- [16] K. S. Jeong, K. Matsukawa, S. Nakagawa, and F. Takahashi, JCAP **03**, 026 (2022), arXiv:2201.00681 [hep-ph].
- [17] S. Nakagawa, F. Takahashi, M. Yamada, and W. Yin, Phys. Lett. B **839**, 137824 (2023), arXiv:2210.10022 [hep-ph].
- [18] L. Di Luzio and P. Sørensen, JHEP **10**, 239 (2024), arXiv:2408.04623 [hep-ph].
- [19] J. E. Kim, Phys. Rev. Lett. **43**, 103 (1979).
- [20] M. A. Shifman, A. I. Vainshtein, and V. I. Zakharov, Nucl. Phys. B **166**, 493 (1980).
- [21] A. R. Zhitnitsky, Sov. J. Nucl. Phys. **31**, 260 (1980).
- [22] M. Dine, W. Fischler, and M. Srednicki, Phys. Lett. B **104**, 199 (1981).
- [23] K. Harigaya, M. Ibe, M. Kawasaki, and T. T. Yanagida, JCAP **11**, 003 (2015), arXiv:1507.00119 [hep-ph].
- [24] A. R. Liddle and R. J. Scherrer, Phys. Rev. D **59**, 023509 (1999), arXiv:astro-ph/9809272.
- [25] S. Borsanyi *et al.*, Nature **539**, 69 (2016), arXiv:1606.07494 [hep-lat].
- [26] G. Grilli di Cortona, E. Hardy, J. Pardo Vega, and G. Villadoro, JHEP **01**, 034 (2016), arXiv:1511.02867 [hep-ph].
- [27] M. Gorghetto and G. Villadoro, JHEP **03**, 033 (2019), arXiv:1812.01008 [hep-ph].
- [28] M. Kawasaki, K. Saikawa, and T. Sekiguchi, Phys. Rev. D **91**, 065014 (2015), arXiv:1412.0789 [hep-ph].
- [29] A. D. Linde, Phys. Rev. D **53**, R4129 (1996), arXiv:hep-th/9601083.
- [30] K. Saikawa and S. Shirai, JCAP **05**, 035 (2018), arXiv:1803.01038 [hep-ph].
- [31] D. H. Lyth, Phys. Rev. D **45**, 3394 (1992).
- [32] T. Kobayashi, R. Kurematsu, and F. Takahashi, JCAP **09**, 032 (2013), arXiv:1304.0922 [hep-ph].
- [33] Y. Akrami *et al.* (Planck), Astron. Astrophys. **641**, A10 (2020), arXiv:1807.06211 [astro-ph.CO].
- [34] C. D. Froggatt and H. B. Nielsen, Nucl. Phys. B **147**, 277 (1979).
- [35] T. Goto and M. Yamaguchi, Phys. Lett. B **276**, 103 (1992).
- [36] G. B. Gelmini, M. Gleiser, and E. W. Kolb, Phys. Rev. D **39**, 1558 (1989).
- [37] Z. Lalak and S. Thomas, Phys. Lett. B **306**, 10 (1993), arXiv:hep-ph/9303250.
- [38] Z. Lalak, B. A. Ovrut, and S. Thomas, Phys. Rev. D **51**, 5456 (1995).
- [39] Z. Lalak, S. Lola, B. A. Ovrut, and G. G. Ross, Nucl. Phys. B **434**, 675 (1995), arXiv:hep-ph/9404218.
- [40] D. Coulson, Z. Lalak, and B. A. Ovrut, Phys. Rev. D **53**, 4237 (1996).
- [41] S. E. Larsson, S. Sarkar, and P. L. White, Phys. Rev. D **55**, 5129 (1997), arXiv:hep-ph/9608319.
- [42] J. R. C. C. Correia, I. S. C. R. Leite, and C. J. A. P. Martins, Phys. Rev. D **90**, 023521 (2014), arXiv:1407.3905 [hep-ph].
- [43] J. R. C. C. Correia, I. S. C. R. Leite, and C. J. A. P. Martins, Phys. Rev. D **97**, 083521 (2018), arXiv:1804.10761 [astro-ph.CO].
- [44] T. Krajewski, J. H. Kwapisz, Z. Lalak, and M. Lewicki, Phys. Rev. D **104**, 123522 (2021), arXiv:2103.03225 [astro-ph.CO].
- [45] D. Gonzalez, N. Kitajima, F. Takahashi, and W. Yin, Phys. Lett. B **843**, 137990 (2023), arXiv:2211.06849 [hep-ph].
- [46] P. W. Graham and S. Rajendran, Phys. Rev. D **84**, 055013 (2011), arXiv:1101.2691 [hep-ph].